

of the intercellular channel. Definition of the specific molecular boundary will require at least an unambiguous assignment of the transmembrane α helices to the four hydrophobic domains in the amino acid sequence. Nevertheless, these three models emphasized that connexon docking involves multivalent interactions of subunits between connexons, which would confer stability in the formation of the intercellular channel and may in part be required for achieving selectivity in the docking process.

References and Notes

- W. R. Loewenstein, *Physiol. Rev.* **61**, 829 (1981).
- F. Ramón and A. Rivera, *Prog. Biophys. Mol. Biol.* **48**, 127 (1986).
- D. C. Spray and J. M. Burt, *Am. J. Physiol.* **258**, C195 (1990).
- E. C. Beyer and R. D. Veenstra, in *Handbook of Membrane Channels*, C. Peracchia, Ed. (Academic Press, San Diego, CA, 1994), pp. 379–401.
- R. Bruzzone, T. W. White, D. L. Paul, *Eur. J. Biochem.* **238**, 1 (1996).
- N. M. Kumar and N. B. Gilula, *Cell* **84**, 381 (1996).
- J. Bergoffen et al., *Science* **262**, 2039 (1993).
- L. J. Bone et al., *Neurobiol. Dis.* **4**, 221 (1997).
- L. Zelante et al., *Hum. Mol. Genet.* **6**, 1605 (1997).
- T. W. White, M. R. Deans, D. P. Kelsell, D. L. Paul, *Nature* **394**, 630 (1998).
- S. H. Britz-Cunningham, M. M. Shah, C. W. Zuppan, W. H. Fletcher, *N. Engl. J. Med.* **332**, 1323 (1995).
- A. G. Reaume et al., *Science* **267**, 1831 (1995).
- J. L. Ewart et al., *Development* **124**, 1281 (1997).
- P. A. Guerrero et al., *J. Clin. Invest.* **99**, 1991 (1997).
- M. Yeager, *J. Struct. Biol.* **121**, 231 (1998).
- P. N. T. Unwin and P. D. Ennis, *Nature* **307**, 609 (1984).
- L. Makowski, D. L. D. Caspar, W. C. Phillips, D. A. Goodenough, *J. Cell Biol.* **74**, 629 (1977).
- L. C. Milks et al., *EMBO J.* **7**, 2967 (1988).
- S. B. Yancey et al., *J. Cell Biol.* **108**, 2241 (1989).
- M. Yeager and N. B. Gilula, *J. Mol. Biol.* **223**, 929 (1992).
- N. M. Kumar, D. S. Friend, N. B. Gilula, *J. Cell Sci.* **108**, 3725 (1995).
- V. M. Unger, N. M. Kumar, N. B. Gilula, M. Yeager, *Nature Struct. Biol.* **4**, 39 (1997).
- Expression and 2D crystallization of α_1 -Cx263T was performed as described in (22), with the following modifications. The sleep-inducing lipid oleamide (34), which has been shown to induce gap junction closure in vivo (35), and the trifluoromethylketone inhibitor of fatty acid amide hydrolase (36) were present during the induction period of the BHK cells at concentrations of 100 and 1 μ M, respectively. Oleamide was added in an attempt to investigate if it caused conformational changes in comparison to our previous projection map. The addition of the inhibitor was necessary because BHK cells showed an oleamide-hydrolyzing enzymatic activity. Because the in vivo effects of the oleamide are reversible, this lipid was also added during all stages of the specimen preparation (100 μ M), the detergent extraction of the membranes (200 μ M), and the final dialysis (100 μ M) of the sample. Stock solutions of oleamide and the trifluoromethylketone inhibitor were prepared in ethanol and added to the growth medium just before use. The final ethanol concentration in the medium was 0.1%.
- Carbon-coated molybdenum grids and frozen and hydrated specimens were prepared as previously described (22). Low-dose electron micrographs of specimens tilted from 0° to 35° were recorded on a Philips CM200FEG microscope at an accelerating voltage of 200 kV, a nominal magnification of 50,000, and defocus values ranging from -2000 to -15,000 Å. Crystal quality was assessed by the optical diffraction of electron micrographs, and only those images with spots visible to a resolution of at least 11 Å were selected for further processing. Micrographs were digitized on a Perkin-Elmer flatbed microdensitometer at a 10- μ m step size (corresponding to 2 Å sampling at the level of the specimen). The MRC image-processing package, which was developed by R. Henderson and colleagues (37–39), was used to analyze the images and to correct for lattice distortions and effects of the contrast transfer function. Initial estimates for the tilt parameter of each crystal were obtained from the changes of the contrast transfer function across the image. Image data were then merged in plane group p6, and lattice lines were fitted with a real-space envelope of 220 Å. Considering only data to a resolution of 15 Å, we refined the tilt geometries of the crystals against a raw 3D model before refining the underfocus values of all images to a resolution of ~7 Å. All images were then processed a second time with back projections of the refined 3D model for the cross-correlation search [R. Henderson, program: MAKETRAN (unpublished program)]. This gave a better description of the lattice distortions and, consequently, a more accurate correction of the image. The improved raw data were subjected to two more cycles of tilt geometry and underfocus refinements, and individual resolution cutoffs were determined for each image before the final merging of data. Density maps were calculated with and without imposing an inverse B factor to ensure that the enhancement of the weak image-derived amplitudes at higher resolution did not introduce spurious density outside the low-resolution molecular boundary. An inverse temperature factor of $B = -350$ was found to be adequate. Application of this sharpening increased the amplitudes at 7.5 Å by a factor of 4.7. The 3D density map was visualized with the program O (40).
- M. Yeager, V. M. Unger, A. K. Mitra, *Methods Enzymol.* **294**, 135 (1999).
- A. Cheng et al., *Nature* **387**, 627 (1997).
- H. Li, S. Lee, B. K. Jap, *Nature Struct. Biol.* **4**, 263 (1997).
- T. Walz et al., *Nature* **387**, 624 (1997).
- M. Auer, C. A. Scarborough, W. Kühlbrandt, *ibid.* **392**, 840 (1998).
- P. Zhang et al., *ibid.*, p. 835.
- C. Elfgang et al., *J. Cell Biol.* **129**, 805 (1995).
- T. W. White, D. L. Paul, D. A. Goodenough, R. Bruzzone, *Mol. Biol. Cell* **6**, 459 (1995).
- C. I. Foote, L. Zhou, X. Zhu, B. J. Nicholson, *J. Cell Biol.* **140**, 1187 (1998).
- B. F. Cravatt et al., *Science* **268**, 1506 (1995).
- X. Guan et al., *J. Cell Biol.* **139**, 1785 (1997).
- B. F. Cravatt et al., *Nature* **384**, 83 (1996).
- R. Henderson et al., *Ultramicroscopy* **19**, 147 (1986).
- R. Henderson et al., *J. Mol. Biol.* **213**, 899 (1990).
- R. A. Crowther, R. Henderson, J. M. Smith, *J. Struct. Biol.* **116**, 9 (1996).
- T. A. Jones, J.-Y. Zou, S. W. Cowan, M. Kjeldgaard, *Acta Crystallogr.* **A47**, 110 (1991).
- D. A. Agard, *J. Mol. Biol.* **167**, 849 (1983).
- G. Perkins, D. Goodenough, G. Sosinsky, *Biophys. J.* **72**, 533 (1997).
- _____, *J. Mol. Biol.* **277**, 171 (1998).
- V. M. Unger and G. F. Schertler, *Biophys. J.* **68**, 1776 (1995).
- We gratefully acknowledge the technical assistance of D. W. Entrikin. This work has been supported by grants from NIH (M.Y. and N.B.G.), the Lucille P. Markey Charitable Trust (N.B.G.), the Gustavus and Louise Pfeiffer Research Foundation (M.Y.), and the Baxter Research Foundation (M.Y.). V.M.U. was a recipient of a postdoctoral fellowship from the American Heart Association. During the course of this work, M.Y. was an Established Investigator of the American Heart Association and Bristol-Myers Squibb and is now the recipient of a Clinical Scientist Award in Translational Research from the Burroughs Wellcome Fund.

29 September 1998; accepted 4 January 1999

Regulation of Neurotrophin-3 Expression by Epithelial-Mesenchymal Interactions: The Role of Wnt Factors

Ardem Patapoutian,^{1*} Carey Backus,² Andreas Kispert,³ Louis F. Reichardt^{1,2}

Neurotrophins regulate survival, axonal growth, and target innervation of sensory and other neurons. Neurotrophin-3 (NT-3) is expressed specifically in cells adjacent to extending axons of dorsal root ganglia neurons, and its absence results in loss of most of these neurons before their axons reach their targets. However, axons are not required for NT-3 expression in limbs; instead, local signals from ectoderm induce NT-3 expression in adjacent mesenchyme. Wnt factors expressed in limb ectoderm induce NT-3 in the underlying mesenchyme. Thus, epithelial-mesenchymal interactions mediated by Wnt factors control NT-3 expression and may regulate axonal growth and guidance.

Neurotrophins are a family of proteins expressed in target tissues that regulate neuronal survival, differentiation, and function (1).

These trophic factors mainly signal through the Trk family of receptor tyrosine kinases that are found on neuronal cell bodies and projections. Gene-targeting experiments have shown that neurotrophins and Trk receptors are required for survival of specific neuronal populations within the peripheral nervous system (1). NT-3 is essential for the survival of most sensory neurons early in development before they reach their final target, at which point they may gain access to target-

¹Department of Physiology, ²Howard Hughes Medical Institute, University of California, San Francisco, CA 94143-0723, USA. ³Department of Molecular Embryology, Max-Planck-Institute for Immunobiology, Stuebeweg 51, D-79108 Freiburg, Germany.

*To whom correspondence should be addressed. E-mail: ardem@itsa.ucsf.edu

REPORTS

derived trophic factors (2, 3). Expression of *NT-3* in early embryos correlates with extending tips of sensory axons en route to their final targets (Fig. 1A) (2). Here, we investigate mechanisms responsible for controlling *NT-3* expression. *NT-3* expression may be induced by axonal tips passing nearby (4), or may be induced through local interactions, independent of neurons and their axonal projections. In this latter model, *NT-3* may have an instructive role in sensory neuron differentiation and pathfinding in vivo (5).

We examined whether sensory neurons are required for *NT-3* expression in one of the main targets of dorsal root ganglia (DRGs), the limb. We developed a whole limb organ culture system using mice heterozygous for the *NT-3^{lacZ}* allele (6). In such mice, the *NT-3* coding region is replaced by the *lacZ* marker gene (7), and X-Gal staining of these mice accurately reflects the endogenous expression of *NT-3* (2). In hindlimb mesenchyme, expression of the *lacZ* marker in *NT-3^{lacZ}* mice begins at embryonic day 11.5 (E11.5), which corresponds to the time when sensory and motor axons invade the limb (Fig. 1, B and C) (2). In hindlimbs of E10.5 mice, X-Gal (Fig. 1B) or neurofilament staining (Fig. 1D) could not be detected. In the absence of neurons, isolated E10.5 hindlimbs cultured for 1 day expressed *lacZ* in a pattern that was spatially indistinguishable from expression in an E11.5 hindlimb (Fig. 1, C and E). Limbs were routinely cultured in 10% fetal bovine serum, but induction of *lacZ* was also observed in the complete absence of serum (8). These results suggest that motor and DRG axons are not required for proper *NT-3* induction in vitro.

To more stringently test the role of sensory neurons in inducing *NT-3*, we crossed the *NT-3^{lacZ}* allele to *spotch* mice (6), which carry a mutation in the Pax-3 transcription factor (9). *Spotch* mice have, among other deficits, a depletion of neural crest cell derivatives, including DRGs (10). In *spotch* embryos, *NT-3* expression at E10 through E14, as assessed by X-Gal staining, appears normal despite the absence of DRG neurons (Fig. 1, F to K) (8). At earlier time points (E10 and E11), when sensory and motor axons are mostly fasciculated, it could be argued that signals from motor neuron axons, which are disorganized but present in *spotch* embryos, can induce *NT-3*. However, by E14, the endings of sensory and motor axons are separated, and the expression of *NT-3* within the dermis, a tissue not invaded by motor neurons, appeared normal in the absence of sensory axons (Fig. 1, H and K). Therefore, these results and those from organ culture argue that *NT-3* induction does not depend on the presence of sensory neurons.

Our data suggest that local interactions, independent of neuronal innervation, are nec-

essary to establish the pattern of *NT-3* expression. To identify the signals that regulate *NT-3* expression, we characterized *lacZ* expression in *NT-3^{lacZ}* mice during embryogenesis. Many of the tissues expressing *NT-3*,

apart from being targets of axons, are also sites of epithelial-mesenchymal boundaries. These domains of expression include limbs, whiskers, hair follicles, kidneys, the digestive system, and arteries (Fig. 2) (2, 11, 12). In

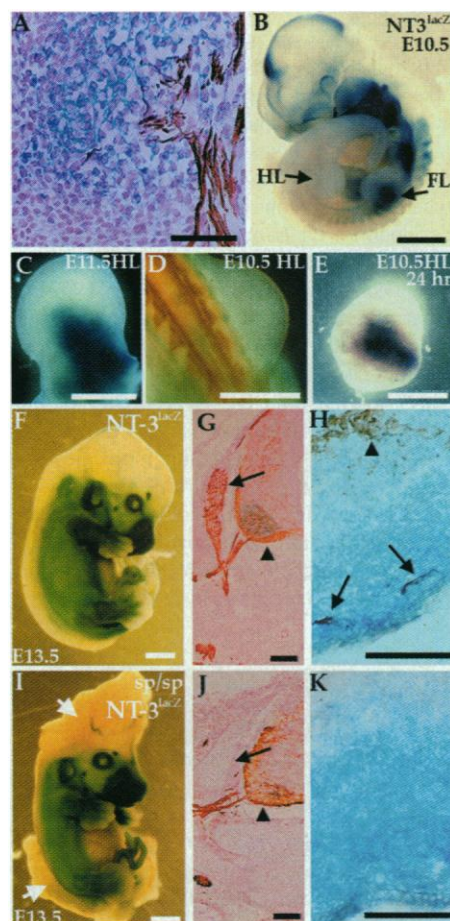


Fig. 1. Expression of *NT-3* in the limb does not depend on innervation. Expression of *NT-3* was detected by a *lacZ* reporter gene stained with X-Gal (blue), and axons were visualized with a neurofilament antibody (NF, brown). (A) E11.5 *NT-3^{lacZ}* embryo section shows colocalization of X-Gal staining with ends of sensory neuron projections. (B) E10.5 *NT-3^{lacZ}* heterozygous embryo shows *lacZ* expression in forelimb (FL) but not hindlimb (HL). (C) E11.5 hindlimb stained for *lacZ* expression. (D) Dorsal view of an E10.5 embryo stained with NF. No axons are present in the hindlimb at this time. (E) E10.5 hindlimb cultured for 24 hours and stained for *lacZ* expression. (F to K) Expression of *lacZ* or NF (or both) in E13.5 *NT-3^{lacZ}* embryos in a wild-type (F to H) or *spotch* background (I to K). Embryos were stained for *lacZ* expression (F and I). The *spotch* embryo exhibits severe defects in the cranial and lumbosacral region (arrows, I). No significant difference in *lacZ* expression in wild-type and mutant embryos is detected. (G and J) NF staining of caudal neural tube sections. DRGs (arrows) are absent in *spotch* mutants, although motor neurons (arrowheads) are present. (H and K) *lacZ*/NF costaining of the distal hindlimb. Sensory (arrows) but not motor (arrowhead) axons correlate with *NT-3* expression as detected by *lacZ* expression (H). (K) *NT-3* expression is normal in the absence of NF staining in *spotch* mice. Bars, 50 μ m (A, H, and K); 1 mm (B, F, and I); 0.5 mm (C to E); 100 μ m (G and J).

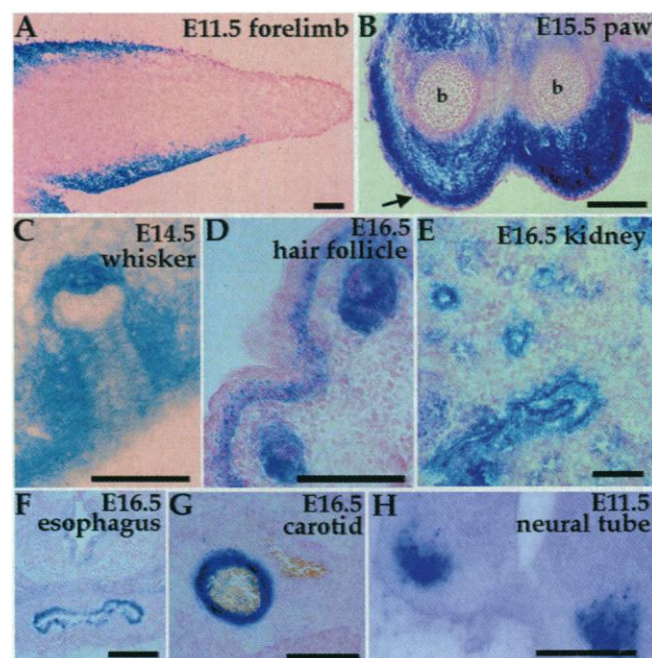


Fig. 2. *NT-3* is expressed in many sites of epithelial-mesenchymal interactions during embryogenesis. X-Gal staining of *NT-3^{lacZ}* heterozygous embryo sections shows expression in (A) E11.5 forelimb mesenchyme, (B) E15.5 forelimb paw [note the absence of expression in ectoderm (arrow) and bone (b)], (C) E14.5 whisker pad, (D) E16.5 hair follicle and skin dermis, (E) E16.5 epithelial cells of the metanephric kidney, (F) E16.5 upper esophagus, (G) E16.5 carotid artery, and (H) motor neurons of E11.5 neural tube. Bars, 100 μ m.

REPORTS

most of these cases, *NT-3* expression was observed in the mesenchyme; however, in the kidney *NT-3* is expressed in the epithelial compartment (Fig. 2E). In the limb, the expression is mainly mesenchymal (Fig. 2, A and B). Embryonic expression of *NT-3* is not confined to sites of epithelial-mesenchymal interactions. For example, within the spinal cord *NT-3* is expressed in motor neurons, a target of central projections of *NT-3*-dependent sensory neurons (Fig. 2H).

To determine whether epithelial signals are important for the induction of *NT-3* in limb mesenchyme, we used the limb organ culture system described above (6). E10.5 hindlimbs from *NT-3^{lacZ}* mice were cultured for 24 to 48 hours with or without ectoderm (13). Our results show that limb ectoderm is necessary for proper mesenchymal expression of *lacZ* in limbs (Fig. 3, A and B). To verify that the *lacZ* induction we observe reflects endogenous *NT-3* expression, we prepared mRNA from limbs cultured for 24 hours with or without ectoderm and analyzed the expression of *NT-3* and γ -actin on a Northern (RNA) blot. Whole limbs showed sixfold higher levels of *NT-3* expression normalized to γ -actin compared with ectodermless limbs (Fig. 3C). The reduced γ -ac-

tin level in the ectodermless sample reflects the fact that limbs without ectoderm were smaller than whole limbs after the culturing period, because of the importance of ectodermal signals for limb outgrowth (14). To ensure that limb mesenchyme was not damaged by ectoderm removal, we replaced the ectoderm of a *NT-3^{lacZ}* limb with wild-type limb ectoderm. When cocultured, the wild-type ectoderm was able to induce *lacZ* expression in the limb mesenchyme after 24 hours (8), and to very robust levels after 48 hours (Fig. 3, D and E). To determine whether *lacZ/NT-3* expression in ectodermless hindlimbs is due to an arrest of limb development under our culture conditions, we removed ectoderm from E10.5 forelimbs, which normally already express *lacZ* (Fig. 1B). After culturing for 24 hours, such limbs did not express *lacZ* (Fig. 3, F and G), suggesting that ectoderm is not simply providing a maturation signal for the limb but is necessary for the induction and maintenance of *NT-3* expression.

To identify the signaling molecules responsible for mediating local induction of *NT-3* expression, we tested different secreted factors of the fibroblast growth factor (FGF), bone morphogenetic protein (BMP), and Wnt families that are expressed in the limb ecto-

derm (14). Beads soaked in FGF-2 or BMP-4 protein did not have detectable *NT-3*-inducing activity on limbs lacking ectoderm (8). To determine whether Wnt proteins can induce *NT-3* expression, we cultured limb mesenchyme without ectoderm in direct contact with cell aggregates from NIH 3T3 cell lines stably transfected with cDNAs encoding different Wnt proteins or with control NIH 3T3 cells (6). Cells expressing *wnt-4*, which is expressed in limb ectoderm (15), induced strong *NT-3* expression in limb mesenchyme (Fig. 4, A and B). Untransfected NIH 3T3 cells or cells expressing *wnt-5a* did not induce detectable *NT-3* expression (Fig. 4, C and D). *Wnt-5a* is mainly expressed in the distal mesenchyme of limbs, a region where *NT-3* is absent (Fig. 2A) (15). Finally, cells expressing *wnt-7a* and *wnt-7b* also induced *NT-3* expression, although to a lesser extent than cells expressing *wnt-4* (Fig. 4, E and F). Both *wnt-7a* and *wnt-7b* are expressed in limb ectoderm, although *wnt-7a* is only expressed in dorsal ectoderm (15). All the transfected cells used in this report express mRNAs encoded by the respective *wnt* genes, and produce Wnts (16); however, without a quantitative comparison of Wnt protein levels, differences in levels of *lacZ* induction cannot be interpreted as significant.

Wnt proteins play crucial roles in development of both invertebrate and vertebrate embryos and have been implicated in human cancer (17). The intracellular components of the Wnt signaling pathway include members of the Frizzled receptor family, glycogen synthetase kinase-3 (GSK3), β -catenin, and the LEF/TCF family of transcription factors that are also highly conserved in evolution. LEF-1 is required for the development of many organs formed by epithelial-mesenchymal interactions (18), and many of these regions express *NT-3*, suggesting a potential direct link between Wnt signaling and *NT-3* expression. *NT-3* is unique among the neurotrophins for its ability to activate all three Trk receptors and to transiently support in vivo multiple classes of newly formed sensory neurons (19). Understanding *NT-3* regulation may thus provide insight into the mechanisms controlling the differentiation and pathfinding of sensory neurons.

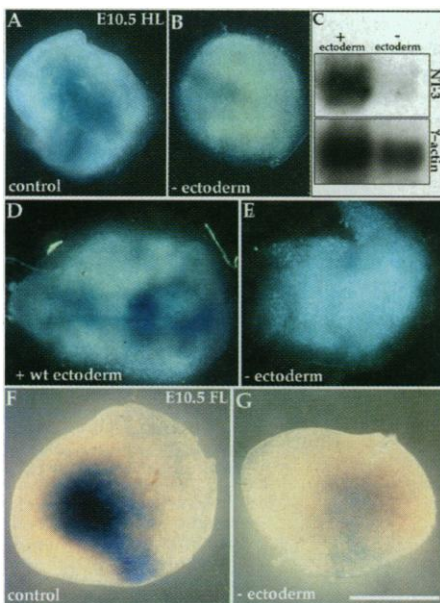


Fig. 3. Ectoderm induces *NT-3* expression in limb mesenchyme. Limbs were isolated from E10.5 *NT-3^{lacZ}* heterozygotes and cultured in vitro. (A) An intact hindlimb expresses *NT-3*, as assessed by X-Gal staining, but (B) a hindlimb lacking ectoderm does not. (C) A Northern blot containing mRNA isolated from limbs cultured with or without ectoderm (10 limbs per lane), probed for *NT-3* and γ -actin. (D) *NT-3^{lacZ}* hindlimb mesenchyme reconstituted with wild-type ectoderm exhibits *lacZ* expression, but (E) a hindlimb lacking ectoderm does not. (F) Forelimb shows strong *lacZ* expression, (G) whereas a forelimb lacking ectoderm does not. All limbs were cultured for 24 hours with the exception of (D) and (E), which were cultured for 48 hours. Bar, 0.5 mm.

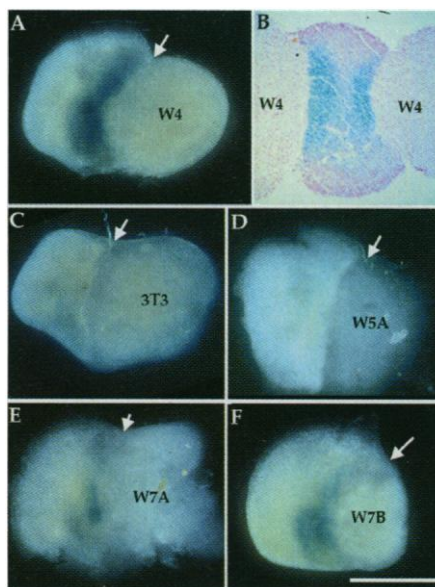


Fig. 4. Wnt proteins are sufficient to induce *NT-3* expression. Mesenchymal hindlimb tissue (without ectoderm) isolated from E10.5 *NT-3^{lacZ}* heterozygous embryos was cocultured with aggregates of NIH 3T3-derived cell lines for 24 hours, after which they were stained with X-Gal. (A) Wnt-4-expressing NIH 3T3 cells induce *NT-3* in limb mesenchyme. (B) A Wnt-4/limb/Wnt-4 explant stained and sectioned shows two blue stripes at the junction of the two tissues. (C) NIH 3T3 cells or (D) Wnt-5a-expressing cells do not induce *NT-3*, whereas (E) Wnt-7a- or (F) Wnt-7b-expressing cells induce *NT-3* to a certain extent. Arrows point to junctions of limb mesenchyme and cell aggregates. Bar, 0.5 mm.

References and Notes

1. L. F. Reichardt and I. Fariñas, in *Molecular Approaches to Neural Development*, M. W. Cowan, T. M. Jessell, L. Zipurski, Eds. (Oxford Univ. Press, New York, 1997), pp. 220-263.
2. I. Fariñas, C. K. Yoshida, C. Backus, L. F. Reichardt, *Neuron* **17**, 1065 (1996).
3. W. M. Elshamy and P. Ernfors, *ibid.* **16**, 963 (1996).
4. J. M. Verdi et al., *ibid.*, p. 515.
5. H. J. Song, G. L. Ming, M. M. Poo, *Nature* **388**, 275 (1997).
6. The generation of *NT-3^{lacZ}* mice has been previously described (7). Embryos were fixed and stained for neurofilament antibody or *lacZ* as described (2). Some sections were counterstained with nuclear Fast Red. *Splotch* mice were obtained from Jackson Lab-

REPORTS

oratories (Bar Harbor, ME). All explants were cultured on 8- μ m polycarbonate filters in Transwell plates (Costar) at the interface of medium (15% fetal bovine serum in Dulbecco's modified Eagle's medium, L-glutamine, penicillin, and streptomycin). For ectoderm separation, tissues were incubated with 6% pancreatin (Gibco-BRL) for 30 min on ice, washed in 10% serum for 20 min, and peeled (13). NIH 3T3 cell lines were aggregated by culture in hanging drops (20). Explant cultures shown are representative of at least four independent experiments. Rat *NT-3* and human γ -actin cDNAs were used as probes for the Northern blot, which was quantified with a multiimager (Fuji).

7. I. Fariñas, K. R. Jones, C. Backus, X. Y. Wang, L. F. Reichardt, *Nature* **369**, 658 (1994).

8. A. Patapoutian and L. F. Reichardt, unpublished observations.

9. D. J. Epstein, M. Vekemans, P. Gros, *Cell* **67**, 767 (1991).

10. T. Franz, *Anat. Embryol.* **187**, 371 (1993).

11. L. C. Schecterson and M. Bothwell, *Neuron* **9**, 449 (1992).

12. G. A. Wilkinson, I. Fariñas, C. Backus, C. K. Yoshida, L. F. Reichardt, *J. Neurosci.* **16**, 7661 (1996).

13. A. Neubüser, H. Peters, R. Balling, G. R. Martin, *Cell* **90**, 247 (1997).

14. R. L. Johnson and C. J. Tabin, *ibid.*, p. 979.

15. B. A. Parr, M. J. Shea, G. Vassileva, A. P. McMahon, *Development* **119**, 247 (1993).

16. A. Kispert, S. Vainio, A. P. McMahon, *ibid.* **125**, 4225 (1998).

17. K. M. Cadigan and R. Nusse, *Genes Dev.* **11**, 3286 (1997).

18. C. van Genderen *et al.*, *ibid.* **8**, 2691 (1994).

19. I. Fariñas, G. A. Wilkinson, C. Backus, L. F. Reichardt, A. Patapoutian, *Neuron* **21**, 325 (1998).

20. T. Serafini *et al.*, *Cell* **78**, 409 (1994).

21. We thank N. Hong, U. Müller, A. Neubüser, and members of Reichardt lab for valuable comments and A. Saulys for technical help. This work was supported by research grants from the U.S. Public Health Service (National Institutes of Health grant MH48200) and the Howard Hughes Medical Institute. A.P. is a fellow of the Damon Runyon-Walter Winchell Cancer Research Foundation and L.F.R. is an investigator of the Howard Hughes Medical Institute.

7 October 1998; accepted 21 January 1999

Reciprocal Control of T Helper Cell and Dendritic Cell Differentiation

Marie-Clotilde Risoan,^{1*} Vassili Soumelis,^{1*} Norimitsu Kadowaki,^{2*} Geraldine Grouard,¹ Francine Briere,¹ René de Waal Malefyt,² Yong-Jun Liu^{1,2†}

It is not known whether subsets of dendritic cells provide different cytokine microenvironments that determine the differentiation of either type-1 T helper (T_H1) or T_H2 cells. Human monocyte (pDC1)-derived dendritic cells (DC1) were found to induce T_H1 differentiation, whereas dendritic cells (DC2) derived from CD4⁺CD3⁺CD11c⁻ plasmacytoid cells (pDC2) induced T_H2 differentiation by use of a mechanism unaffected by interleukin-4 (IL-4) or IL-12. The T_H2 cytokine IL-4 enhanced DC1 maturation and killed pDC2, an effect potentiated by IL-10 but blocked by CD40 ligand and interferon- γ . Thus, a negative feedback loop from the mature T helper cells may selectively inhibit prolonged T_H1 or T_H2 responses by regulating survival of the appropriate dendritic cell subset.

The cytokine microenvironment plays a key role in T helper cell differentiation toward the T_H1 or T_H2 cell type during immune responses (1-6). IL-12 induces T_H1 differentiation, whereas IL-4 drives T_H2 differentiation. Because T helper cell differentiation requires the presence of different cytokines at an initial stage of the T cell-dendritic cell (DC) interaction (1-7), we investigated whether distinct DC lineages or subsets may produce different cytokines and directly induce T_H1 or T_H2 differentiation.

Humans have two distinct types of DC precursors. Peripheral blood monocytes (designated pDC1) give rise to immature myeloid DCs after culturing with granulocyte-macrophage colony-stimulating factor (GM-CSF) and IL-4 (8-10) or after transmigration through endothelial cells and phagocytosis (11). These immature cells become mature myeloid DCs (designated DC1) after stimulation with CD40 ligand (CD40L) or endotoxin (12, 13). The CD4⁺CD3⁺CD11c⁻ plasmacytoid cells (designated pDC2) from blood or tonsils give rise to a distinct type of immature DC after culture with IL-3 (14-16). These cells differentiate into mature DCs (designated DC2) after CD40L stimulation (17). However, unlike pDC1 and DC1, pDC2 and DC2 display features of the lymphoid lineage: (i) pDC2 and DC2 express few myeloid antigens, such as CD11b, CD11c, CD13, and CD33 (14); (ii) pDC2 cells do not differentiate into macrophages, following culture with GM-CSF and M-CSF; (iii) pDC2 and DC2 have little capacity to phagocytose or macropinocytose antigens at all stages of their maturation (14) (iv) like the putative mouse lymphoid DCs (18), pDC2 cells depend on IL-3, but not GM-CSF for their survival and maturation (14) [this can be explained by high GM-CSF receptor and low IL-3 receptor expression in pDC1 cells and low GM-CSF receptor and high IL-3 receptor expression in pDC2 cells (Fig. 1)]; and (v) pDC2 cells have high levels of pre-T cell receptor α -chain expression (19).

Both myeloid DC1 and "lymphoid" DC2 induce strong proliferation of allogeneic naïve

CD4⁺ T cells (14). First, we examined the profile of cytokine production from DC1 and DC2 after CD40L activation. DC1 produced large amounts of IL-12 within 24 hours after CD40L activation (Fig. 2) as reported (12, 13), whereas DC2 did not (Fig. 2). In addition, unlike CD40L-activated DC1, CD40L-activated DC2 produced little IL-1 α , IL-1 β , IL-6, and IL-10, but produced comparable amounts of chemokine IL-8 (Fig. 2) (20). Neither CD40L-activated DC1 nor DC2 produced detectable amounts of IL-4 and IL-13. Quantitative polymerase chain reaction (PCR) analyses showed that CD40L activation up-regulated the expression of mRNA for IL-12p40, IL-1 α , and IL-1 β in DC1, but not in DC2 (Table 1) (21). Neither DC1 nor DC2 transcribed detectable amounts of IL-4 mRNA, either before or after CD40L activation (Table 1).

We next examined the nature of primary allogeneic T cell responses induced by DC1 or DC2. Naïve CD4⁺CD45RA⁺ T cells isolated from human peripheral blood or umbilical cord blood were cocultured for 7 days with CD40L-activated DC1, CD40L-activated DC2, or antibodies to CD3 and CD28 (22). The cultured cells were counted and restimulated with anti-CD3 and anti-CD28 for either 4 hours for single-cell cytokine analyses by flow cytometry (Fig. 3B) or 24 hours for cytokine secretion analyses by enzyme-linked immunosorbent assay (ELISA) (Fig. 3A). T cells originally cul-

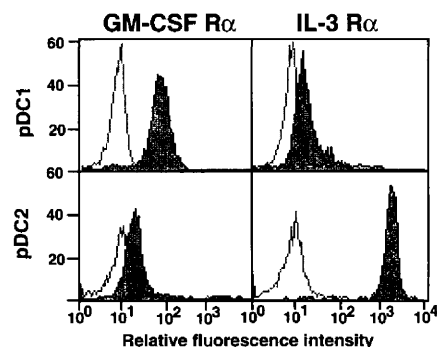


Fig. 1. Expression of GM-CSF receptor α chain (GM-CSF R α) and IL-3 receptor α chain (IL-3 R α) on pDC1 and pDC2 (open curve, isotype control; shaded curve, specific staining).

¹Schering-Plough, Laboratory for Immunological Research, 27 chemin des Peupliers, Boite Postale 11, 69571, Dardilly, France. ²DNAX Research Institute of Molecular and Cellular Biology, 901 California Avenue, Palo Alto, CA 94304-1104, USA.

*These authors contributed equally to this work.

†To whom correspondence should be addressed. E-mail: yliu@dnax.org